Egyptian Journal of Chemistry

http://ejchem.journals.ekb.eg/

Synthesis and spectroscopic characterization of dimer, mono- and bi-nuclear copper complexes of 2-[α-(acetyloxime) ethylidene hydrazino]-4,6-dimethylquinoline

Fatma Samy*, Magdy Shebl, Ali Taha, H.S. Seleem

Department of Chemistry, Faculty of Education, Ain Shams University, Roxy, Cairo 11341, Egypt

Abstract

2-[α-(acetyloxime)ethylidenehydrazino]-4,6-dimethylquinoline (MHQ) and its Cu complexes have been synthesized and characterized by elemental analysis and electronic, vibrational, electron, spin resonance and mass spectra. The mononuclear, binuclear and dimeric chelates have been isolated by reaction of the ligand with different Cu^{II} salts (nitrate, perchlorate, sulfate, acetate, chloride and bromide) in addition to Cu^{I} iodide) in molar ratio 1:1 and 1:2 (metal:ligand). The results showed that the ligand acts as bidentate (NN or NO) and tridentate (NNN or NNO). Multilinear regression analysis (MLRA) of the d–d transitions of Cu-MHQ complexes in different solvents *vs.* Guttmann parameters (AN, DN and ε) and solvato parameters (α, β and π*) have been determined. Full geometrical and structural optimizations of the ligand and its metal complexes have been performed by a *PM3* study by using the hyperchem program.

Keywords: Quinoline, hydrazones, copper complexes, molecular modeling, ESR spectra.

1. Introduction

For decades, hydrazones and their metal complexes have attracted a great interest because of their excellent applications and biological activities such as antibacterial, antioxidant, anticonvulsant, anti-inflammatory, antifungal, antidepressant, antiviral analgesic, antimalarial, antiplatelet, antimycobacterial and vasodilator and antitumor.[1-7] Quinoline-based compounds have different important pharmacological activities.[8-13] Also, the quinoline ligands form important complexes, which have many applications at different fields. Oximes play an important role in development of coordination chemistry due to their versatile bonding.[14,15] The current work is an extension to our previous studies including quinoline-based complexes[16-24] and our interest in investigation of the effect on anions on complexation[25], especially for Cu(II) complexes.[26-28] Thus, we anticipated that the interaction of the oximic MHQ hydrazone with Cu^{II} ions would create novel complexes. Based on the foregoing facts and in an attempt to investigate the effect of anion of the metal salt on the formed chelates, a new hydrazone ligand; MHQ (H_2L) was synthesized and allowed to react with several Cu^{II}-salts e.g. NO_3^-, ClO_4^-, AcO^-, SO_4^{2-}, Cl^- and Br^- in

addition to Cu^{I} as CuI. The ligand and its copper complexes were characterized by elemental analysis and electronic, vibrational, electron spin resonance and mass spectra. These reactions afforded mononuclear and binuclear complexes including paramagnetic and diamagnetic complexes. In another attempt, the MHQ was allowed to react with Cu^{II}–nitrate in presence of triethyl amine (NEt_3) in methanol, (1 : 1 : 1; Cu^{II} / MHQ / NEt_3). This reaction afforded a dimeric complex **7** with no sign for adduct formation (Scheme 2) i.e. a base catalyzed dimerization occurs. In addition, multilinear regression analysis (MLRA) of the d–d transitions of Cu-MHQ complexes in different solvents *vs.* Guttmann parameters (AN, DN and ε) and solvato parameters (α, β and π*) have been determined. The structural optimizations of the ligand and its metal complexes have been performed by a *PM3* study by using the hyperchem program.

2. Experimental

2.1 Materials

Nitrate, perchlorate, sulfate, acetate, chloride and bromide of Cu^{II} in addition to Cu^{I} iodide, disodium salt of EDTA, organic solvents, *p-*

toluidine, ethyl acetoacetate, phosphorus oxychloride, hydrazine hydrate, biacetylmonoxime, trimethylamine, hexamine and murexide were Merck, BDH, Aldrich and Fluka.

2.2 Preparation of hydrazone

The preparation of 2-hydrazino-4,6-dimethylquinoline (HQ) is described in our previous publication.[16,24] The mixture of HQ (0.01 mol.) with biacetylmonoxime (0.01 mol.) was heated under reflux for 1/2 hour. After cooling, the yellow monoxime ligand, 2-[α-(acetyloxime)ethylidenehydrazino]-4,6-dimethylquinoline (MHQ) (Scheme 1) was filtered off, washed with ether and the crystallization is performed by using ethanol. Table 1 showed elemental analysis, and colour of the ligand; 80 % yield; m.p 256 °C.
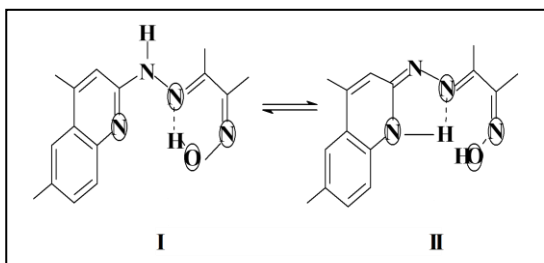
**Scheme 1.**Tautomric structure of the MHQ ligand.

2.3 Preparation of the complexes

Methanolic solutions of the metal salts (1 mmol) were added with constant stirring to the methanolic solution of MHQ hydrazone (1 or 2 mmol). The reaction mixture was heated under reflux for *ca* 5 – 7 hours on a water bath. The precipitated solid complex (Scheme 2) was filtered off, washed several times with methanol and finally washed with diethyl ether and then dried in *vacuo*, yield ≈ 60 – 80 %.

2.4 Measurements

IR spectra (4000-400 cm^{-1}) were recorded on a BRUKER Vector 22 spectrometer (Germany) using KBr pellets. UV-Visible spectra were recorded on a Jasco V-550 UV/VIS spectrophotometer. Mass spectra were recorded at 70 eV on a gas chromatographic GCMSqp 1000-ex Shimadzu mass spectrometer. ESR spectra were recorded on Bruker Elexsys, E500 operated at X-band frequency. Molar conductance's of millimolar solutions of the solid complexes in DMF were measured on the Corning conductivity meter NY 14831 model 441 (USA). Magnetic susceptibilities of the complexes were measured by the Gouy method at room temperature using a Johnson Matthey Alfa MKI magnetic susceptibility balance with Hg[Co(CNS)₄] as a

calibrant. The effective magnetic moments were calculated from the expression $\mu_{eff.} = 2.828\,(\chi_M.T)^{1/2}$ BM, where χ_M is the molar susceptibility corrected using Pascal's constants for the diamagnetism of all atoms in the compound. Microanalyses of carbon, hydrogen and nitrogen were carried out on W. C. Heraeus Hanau elemental analyzer and Perkin-Elmer 2400 CHN elemental analyzer. The melting point of the ligand and decomposition temperatures of the complexes were determined using Rumo-3600 melting point apparatus.
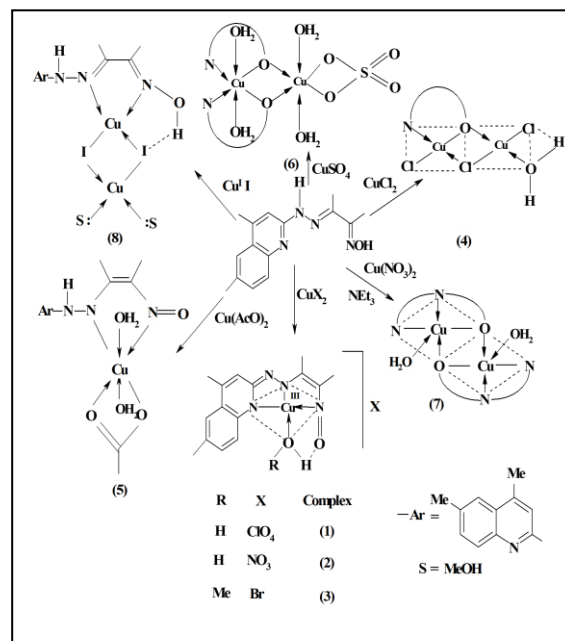
Scheme 2. Metal complexes of the MHQ ligand.

2.5 Molecular orbital calculations

The optimized structures of hydrazone ligand and its metal complexes were done by Hyperchem 7.52 program, using *PM3* level.

3. Results and discussion

3.1. Characterization of the ligand

IR spectrum of the ligand (Table 2) showed strong to medium broad characteristic bands at 3336, 2917 and 1610 cm^{-1} for the ligand. These bands refer to the stretching vibrational modes of NH, OH---N and C=N (azomethine), respectively. The mass spectrum of the MHQ ligand (Fig. 3a) showed molecular ion and base peaks at *m/z* 305 and 172, respectively, which is in an agreement with its formula weight. Scheme 3. shows the mass fragmentation patterns of MHQ. Three bands at 234, 309 and 355 nm appeared at the electronic absorption spectrum of the oxime ligand. These bands may be assigned to π - π* transitions of the quinoline ring,[16] phenyl rings and/or azomethine groups,[4a,7,24b] charge transfer (CT) and the low

intensity n - π^* forbidden transitions, respectively.[29] The elemental analysis data and spectral studies confirm the structure of MHQ.

3.2. Characterization of the metal complexes

The coordinating sites of MHQ are the nitrogens of the quinoline ring, azomethine linkage and oximic group in addition to the oximic oxygen (Scheme 1).

The MHQ hydrazone (H_2L) was allowed to react with all metal ions used in the mole ratio 1:1; metal ion: ligand. Also, the mole ratio 1:2; metal ion: ligand was tried, but always afforded the same products as in 1:1 ratio. The results of elemental analyses (Table 1) agreed well with the proposed formula.

The isolated solid complexes are colored (green – brown), stable in atmospheric air, non-hygroscopic, and insoluble in water and diethyl ether, but partially soluble in alcohols (methanol and ethanol) and completely soluble in DMF and DMSO. Also, most complexes have high melting points, > 300 °C (an exception: the acetato complex **5**, m.p. ≈ 162-164 °C), indicating their strong bonds and high thermal stability.

The reaction of the hydrazone (H_2L) with the various copper salts afforded dimeric complexes (**7**), binuclear complexes (**4**, **6** and **8**) and mononuclear complexes (**1-3** and **5**). To our findings, in the present study, the complexes formed *via* oximato bridges complexes.[14,15a] The chemistry of oximes has recently been reviewed.[14] It has now become apparent that the bridging ability of the oximato ligands is more readily accessible than was previously thought[14, 15a] i.e. the oximato group (=N-O^-) can function as a bridge to bind two metal ions in various ways.[14,15] The coordinating ability of the SO_4^{2-} anions in complex **6** was checked by $BaCl_2$ solution, where no white precipitate is observed which is compatible with the molar conductance data (Table 3).

3.2.1. IR spectra

The main IR absorption bands for the synthesized complexes are shown in Figs. 1a-1b and Table 2. The observed bands may be classified into those originating from the ligands, those emanating from the counter-balancing anions and those arise from the bonds formed between metal ions and coordinating sites. The mode of bonding of the ligand with different copper salts was investigated by comparing the IR spectra of the solid complexes with that of the free ligand (Table 2).

Inspection of the data (Table 2) reveals the following:

(i)   All complexes exhibit a broad band centered at 3474 - 3394 cm^{-1} which is attributed to $\nu(OH)$ of water and /or methanol molecules associated with complex formation.[4a,7,24b,30]

(ii)   The band located at 3336 cm^{-1} due to $\nu(NH)$ of the free ligand disappeared or overlapped with $\nu(OH)$ for all complexes.

(iii) The strong band located at 1610 cm^{-1} ($\nu C = N$, azomethine) of the free ligand was shifted by ± 13 cm^{-1} as a result of complexation.[24b,30,31-32] This can guide to assume the participation of the azomethine group in chelation through resonating phenomena.

(iv)   The absorption bands with variable intensity in the frequency range 1585 - 1415 cm^{-1} corresponding to the quinoline ring vibrations of the free ligand are highly altered as a result of complexation.

(v)   For most complexes, the broad band centered at 2917 cm^{-1} assignable to $\nu(OH ---- N)$ of the oximic group of the free MHQ ligand disappeared, indicating proton displacement by the metal ions and hence a covalent linkage.

(vi)   The ionic character of the NO_3^- anion in complex **2** was supported by appearance of a new band around 1384 cm^{-1} (Table 2).[33] This is consistent with the conductance measurements.[1]

(vii) The ionic character of the ClO_4^- anion (T_d–symmetry) in complex **1** was achieved by the strong broad splitted bands at ≈ 1108 and 1078 cm^{-1}(ν_3) and the weak band at 928 cm^{-1}(ν_4).

(viii) In the sulfato complex **6**, the strong chelating bidentate ability of the SO_4^{2-} group was supported by the appearance of ν_3(S–O) stretching band at 1148 cm^{-1}, in addition to ν_1(S–O) weak band at 879 cm^{-1}, (Table 2). This provides strong evidence that the high T_d–symmetry of the SO_4^{2-} ion is lowered by complex formation.[26a]

(ix)   In the acetato complex **5**, the two bands at 1573 cm^{-1} ($\nu C=O$) and 1516 cm^{-1} ($\nu C-O$), suggest the bidentate chelating fashion of the acetate ion.[34-35] The separation of these bands, $\Delta\nu = 57$ cm^{-1} is comparable to the cited values[34-35] for the bidentate character of the AcO^- group. It is evident that the ν(C=N, quinoline) may be overlapped with ν(COO^-) of the acetate group (Table 2).

(x)   Support of the above interpretation is the appearance of the non – ligand bands in the ranges 580-540 cm^{-1}, ν(M-O) and 540-480 cm^{-1}, ν(M-N).[7,24b,30,36]

3.2.2. Conductance measurements

Molar conductances of millimolar solutions of complexes in DMF were determined at room temperature (Table 3). The molar conductance for complexes **1–3** shows values of 79 - 65 ohm^{-1} cm^2 mol^{-1}, within the expected range for 1:1 electrolytes, indicating that the NO$_3^-$, ClO$_4^-$ and Br$^-$ anions are not coordinated to the metal ions.[7a]

The chloro (**4**) and iodo (**8**) complexes showed a certain degree of conductivity, $\Lambda = 41$ and 39 ohm^{-1}cm^2 mol^{-1}, respectively. This could be explained on the basis of partial solvolysis[6,37] of the complexes by DMF molecules i.e. an exchange between DMF molecules and the coordinated Cl$^-$ or I$^-$ ions. On other hand, the molar conductance values of the other complexes show low values (4 - 13) ohm^{-1} cm^2 mol^{-1}, suggesting the absence of the ionic character.[4a,7,24b,30 38,39]

3.2.3. Electronic spectra and magnetic studies

The electronic spectra as well as the magnetic susceptibilities (Table 3) of the complexes provide a diagnosis of their stereochemistry. As we have mentioned before, MHQ was allowed to react with several Cu^{II}-salts (NO$_3^-$, ClO$_4^-$, AcO$^-$, SO$_4^{2-}$, Cl$^-$ and Br$^-$) in addition to Cu^I as Cu I (Scheme1). In case of Cu^{II}–perchlorate, the reaction was carried out by refluxing or stirring at room temperature.

Based on the magnetic moment data at room temperature for copper complexes (Table 3), the complexes could be classified into two main categories:

➢ Diamagnetic for complexes **1–3** (Cu^{III}-complexes) and **8** (Cu^I- complex).

➢ Paramagnetic for complexes **4–7**, these complexes have magnetic moments within the range 0.88 – 1.62 μ_β/Cu^{II} ion indicating the presence of one unpaired electron-d^9 system.

➢ The dimeric and binuclear complexes **4**, **6** and **7** have a subnormal magnetic moment (0.88 - 1.05) suggesting a strong antiferromagnetic exchange interaction

between the Cu^{II}–ions of the crystal i.e. the possibility of spin–coupled system or intermolecular interaction.[4a,24b,40]

The electronic spectra of Cu^I–complex (**8**) in DMF showed no d–d transitions as expected for d^{10}–system and the pale brown color of the complex is dominated by a charge transfer transition from ligand to Cu^I–ion; band at 331 nm. However, this band was observed at 433 nm in Nujol mull. Also, the Cu^I-complex **8** has a T$_d$ geometry as expected for d^{10}-systems.

Due to Jahn – Teller effect and because of the low symmetry of the environment around Cu^{II}-ion (d^9), detailed interpretations of the spectral and magnetic data are somewhat complicated.[41-42] The electronic spectra of Cu^{II}–complexes (**4–6**) showed a charge transfer band (L $\rightarrow$ Cu^{2+}) in the region 331-449 nm as a result of complex formation. In addition, a d–d transition band in the region 500 - 596 nm which can be assigned to $^2B_{1g} \rightarrow {}^2E_g$ transition of the Cu^{II}–ion in tetragonally elongated octahedron or square planar geometry.[43-44] The wine red color of the dimeric complex **7**, [Cu^{II}L(H$_2$O)]$_2$ is dominated only by a charge transfer transition from the deprotonated hydrazone to Cu^{II}-ions; band at 462 nm (Table 3).

The green Cu^{III}-MHQ complexes **1** and **2** showed the spin allowed d–d transition at $\approx$ 509 nm (612 and 628 nm in Nujol mull) which is close to those reported for square planar Cu^{III}–complexes.[45-46] On the other hand, the reddish brown color of Cu^{III}–MHQ complex **3** is dominated only by a charge transfer band at $\approx$ 340 nm (no d–d transition in the measured range).

3.2.4. ESR spectrometry

The ESR spectrum of complex **2** (Fig. 2) showed a sharp isotropic signal at g$_{iso}$ = 2.04 which may be attributed to a conduction ESR band of metallic copper.[53] The presence of metallic copper (Cu^0) species could be explained on the basis of one electron transfer between the copper species as shown below:

3 Cu^{2+} $\rightarrow$ 2 Cu^{3+} + Cu^0
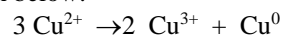
The pattern of the g - value together with the shape of the ESR signal are comparable to those reported in literature for Cu^0.[45] On the other hand, the ESR spectrum of the dimeric complex **7** (Fig. 2) showed a considerable broad isotropic signal at g$_{iso}$ = 1.95. This broadening accounts for: i) Equal and high symmetry around the two Cu^{II}-ions. ii) Electron delocalization in the formed chelate rings.

Table1. Analytical and physical data of the MHQ complexes.

No.	Complex (M. F.)	F.Wt	Color	Elemental Analysis; % Found/(Calc.)			
				C	H	N	M
	MHQ $C_{15}H_{18}N_4O$	270	Yellow	66.40 (66.66)	6.50 (6.60)	20.72 (20.74)	-----
1	$[Cu^{III}L(H_2O)]ClO_4$ $CuC_{15}H_{18}N_4O_6Cl$	449	Green crystals	39.92[a] 40.61[b] (40.09)	4.66[a] 3.99[b] (4.01)	12.63[a] 11.97[b] (12.47)	----- (14.14)
2	$[Cu^{III}L(H_2O)]NO_3.MeOH$ $CuC_{16}H_{22}N_5O_6$	443.5	Green crystals	43.77 (43.29)	5.37 (4.96)	16.84 (15.78)	----- (14.32)
3	$[Cu^{III}L(MeOH)]Br$ $CuC_{16}H_{20}N_4O_2Br$	443.4	Reddish-Brown	42.95 (43.30)	4.43 (4.51)	----- (12.63)	----- (14.32)
4	$[Cu_2^{II}(HL)Cl_3(H_2O)]$ $Cu_2C_{15}H_{19}N_4O_2Cl_3$	520.5	Green	34.69 (34.58)	3.56 (3.65)	10.26 (10.76)	23.75 (24.40)
5	$[Cu^{II}(HL)AcO(H_2O)_2]$ $CuC_{17}H_{24}N_4O_5$	427.5	Reddish-Brown	48.03 (47.72)	5.17 (5.61)	11.46 (13.10)	13.75 (14.85)
6	$[Cu_2^{II}(HL)_2SO_4(H_2O)_4].2½ H_2O$ $Cu_2C_{30}H_{47}N_8O_{12.5}S$	878	Green	40.95 (41.00)	5.08 (5.35)	12.53 (12.76)	14.00 (14.46)
7	$[Cu^{II}L(H_2O)]_2$ $Cu_2C_{30}H_{36}N_8O_4$	699	Wine Red	51.48 (51.50)	4.67 (5.15)	15.76 (16.02)	17.95 (18.17)
8	$[Cu_2^I(H_2L)I_2(MeOH)_2].MeOH$ $Cu_2C_{18}H_{30}N_4O_4I_2$	747	Pale brown	29.43 (28.92)	3.52 (4.02)	8.71 (7.50)	----- (17.00)

* 1[a] by reflux and 1[b] by stirring.

Table 2. Selected IR absorption bands (cm^{-1}) of the MHQ complexes.

Complex	IR spectral bands cm^{-1}			
	νNH/OH(OH group or H$_2$O or methanol)	ν(C = N) free / coord.	ν(C = N) (quinoline)	Other bands
H$_2$L	3336	1610	1579, 1497, 1452, 1403	2917; OH….N
1[a]	3474	1609	1534, 1444	(1108, 1078); ν$_3$(Cl-O)
1[b]	3474	1607	1540, 1442	
2	3425	1612	1539,1505	(1407, 1385); ν(NO$_3^-$)
3	3446	1606	1584, 1517, 1460	
4	3418	1611	1530, 1415	
5	3419	1600	…….	1573; ν$_{as}$(COO$^-$), 1516; ν$_s$(COO$^-$)
6	3426	1611	1539, 1498	(1148, 1120, 1094); ν$_3$(S-O)
7	3394	1623	1579, 1546	
8	3425	1608	1585, 1519, 1457	

* 1[a] by reflux and 1[b] by stirring.
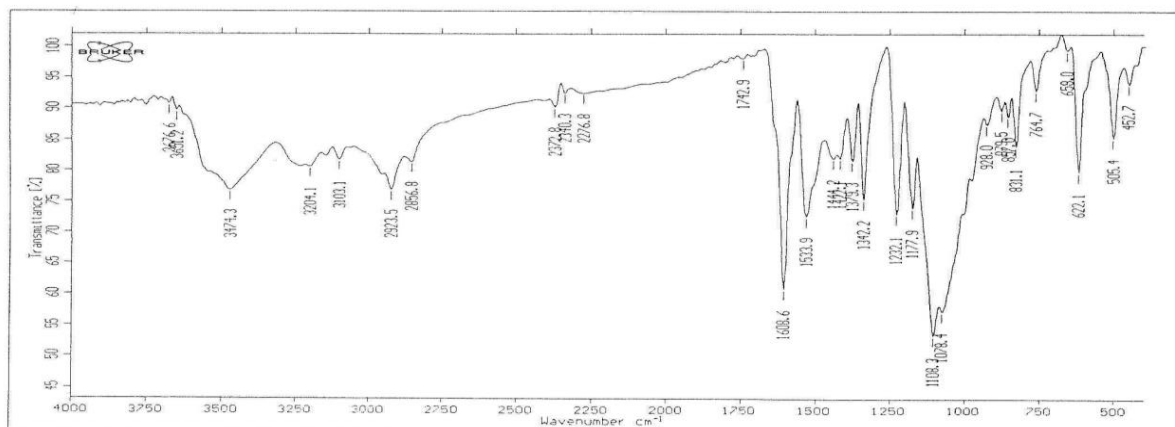
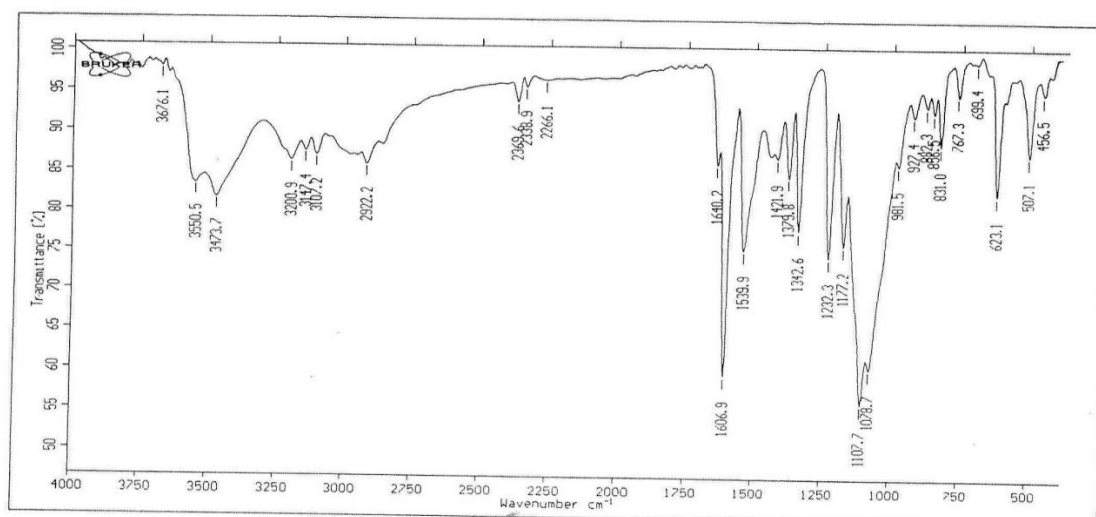**Fig. 1a.** IR spectrum of $[Cu^{III}L(H_2O)].ClO_4$ (1[a]) by reflux.

Fig. 1b. IR spectrum of $[Cu^{III}L(H_2O)].ClO_4$ (1^b) by stirring.

Table 3. Electronic spectra, magnetic moments and molar conductivity data of the MHQ complexes.

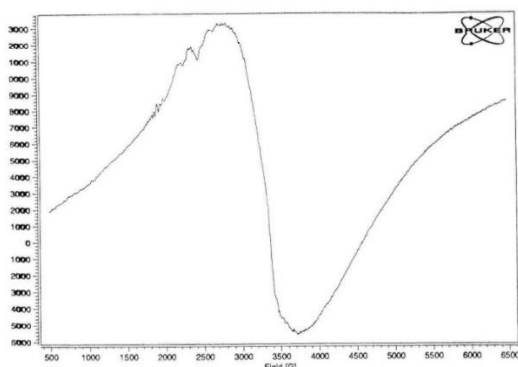| No.	λ_{max} (nm) (DMF)	λ_{max} (nm) Nujol mull	μ_{eff} ($\mu_{comp.}$) μ_β	Λ Ohm^{-1} cm^2 mol^{-1}
H₂L	234, 309, 355	----	---	----
1	509^a, 330, 268	612, 440, 320	Diamagnetic^a	70
	509^b, 331, 267	612, 442, 320	Diamagnetic^b	67
2	509, 326, 268	628, 440, 325	Diamagnetic	79
3	340, 271	334	Diamagnetic	65
4	384	596, 415	0.88 (1.25)	41
5	500, 331	502	1.62	10
6	509, 449	449	1.05 (1.48)	6.0
7	462, 334	465, 352	1.05 (1.49)	4.0
8	331	433	Diamagnetic	39

* 1^a by reflux and 1^b by stirring.

Fig. 2. ESR spectrum of $[Cu^{II}L(H_2O)]_2$ (7).

3.2.5. Mass spectrometry

Mass spectrometry begins by ionizing a sample and the resultant ions are separated and then plotted as a ratio of mass-to-charge; *m/zvs.* % relative abundance. Figs. 3 show the mass spectra of complexes **1**, **2**, and **7**, as representative examples. The molecular ion peaks (F.W.) as well as the base peaks are shown below:

Complex	1	2	7
Molecular ion peak	449	441	698.2
Cacld. F.W.	449	443.5	699
Base peak	272	252	172

Obviously, the molecular ion peaks agree well with the F.W. of the complexes. However, the differences between found and calculated *m/z* values are due to the effect of isotopes. Also, it is obvious that the most abundant ions i.e. the more stable species (the base peak) for Cu^{III}-complexes (**1** and **2**) have the highest *m/z* values (272 and 252 amu, respectively) which correspond to the following charged species:

Hence, this indicates the highest stability of Cu^{III}-complexes.

On the other hand, complex **7** showed the base peak at *m/z* = 172. This provides strong evidence that the most abundant species (more stable species) contains the quinoline ring and corresponds to the following charged species.
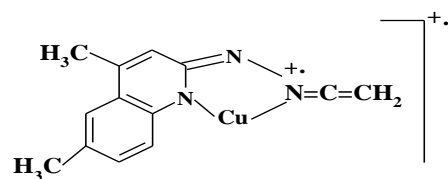
Base peak *m/z* 272 (273.5); complex 1

$-HC \equiv CH$
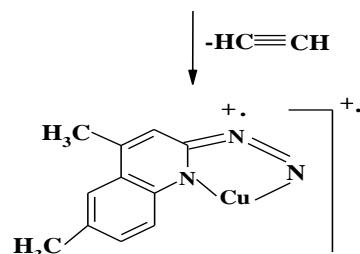
Base peak *m/z* 252 (247.5); complex 2
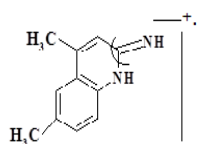
Base peak *m/z* 172 (172); complex 7

-HCN   -·CH₃

m/z   149 (145)   157 (157)
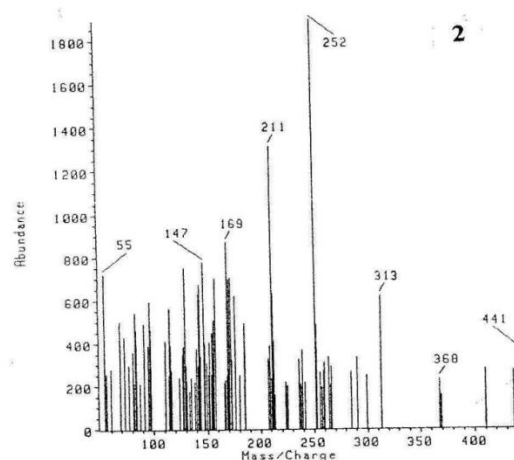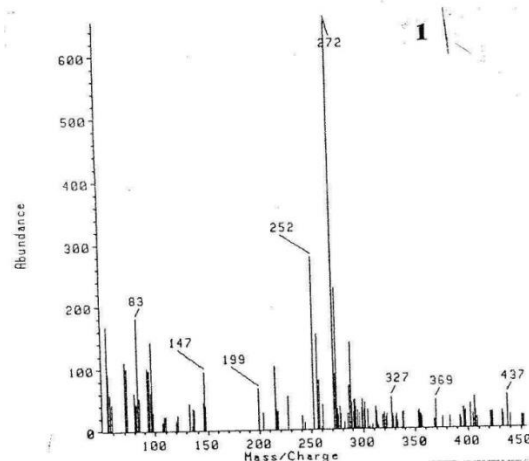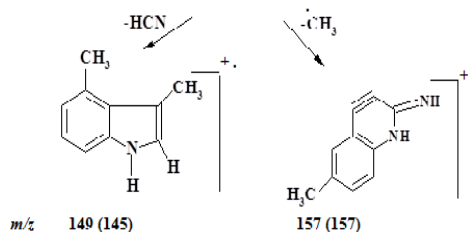
Fig. 3b. [Cu^{III}L(H$_2$O)].ClO$_4$ (**1**) and [Cu^{III}L(H$_2$O)].NO$_3$.MeOH(**2**).

In general, the fragmentation patterns of the complexes show similar fragments to those of the free MHQ hydrazone i.e. the fragmentation patterns detect the places at which the ligand or the complex prefers to fragment. Finally, the molecular ion peaks confirmed the proposed formulae of the complexes.

The arguments supporting the Cu^{III}-MHQ structure (**1**-**3**) begin with the observation that a diamagnetic complex was obtained as well as the analytical and spectral data (Tables 1 & 3). The evidences that support the Cu^{III}-structure can be summarized in the following:

(i)   Diamagnetism indicates either Cu^{I}-structure with d^{10} configuration or Cu^{III}-structure with d^{8}–configuration[46-47] (square planar) similar to that of Ni^{II}-square planar;

Cu^{I} ←[Reduction / +e$^-$]   Cu^{II} →[Oxidation / -e$^-$]   Cu^{III}

(d^{10} - Diamagnetic)   (d^9 - Paramagnetic)   (d^8 - Square planar Diamagnetic)
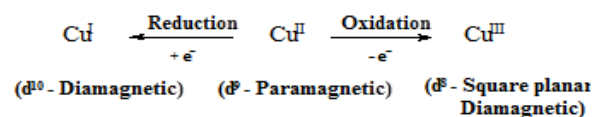
(ii)   The electronic spectra (Table 3) showed one spin - allowed d-d transition at ≈ 509 nm with a high ε value indicating an appreciable covalency in the Cu - N bonds.[48] This is compatible with square

Fig. 3a. Mass spectra of MHQ, ligand.

planar d^8-systems. Also, two additional intense bands at $\approx$ 440 and 320 nm were observed which may be assigned to L → Cu^{III} CT and intra - ligand transitions.

(iii)   The results of elemental analysis as well as the mass spectra are coincident completely with the suggested structures.

(iv)   The lack of ESR signal characterized for Cu^{II}-square planar complexes (see Fig. 2).[48]

Other considerations:

➢   It is well known that all Cu^{III}-complexes are diamagnetic with square or five-coordination of Cu^{III} (an exception; K_3CuF_6).[41]

➢   It was found that Cu^{III} is stabilized by tetradentate imine-oxime ligands[48-51] which are similar to the MHQ ligand; hydrazone-oxime.

➢   Also, it was found that Cu^{III}-complexes with 5- membered chelate rings - similar to that obtained in our case - are independent of pH.[48] This supports our interpretation.[49]

(v)   The stabilization of the higher oxidation states of transition metal ions; silver(III), copper(III), nickel(III, IV) and cobalt(IV) by oximic ligands is attributed to both the π-donor character of the oxime group and the negative charge on the oximato-oxygen which partially neutralizes the positive charge on the metal ion.[50] In general, Cu^{III}-complexes have an important role in biological redox systems such as galactose oxidase[51-53], where Cu^{III} is reduced to Cu^{I}.

3.2.6. Spectrophotometric studies on the metal chelates of MHQ ligand

Metallic complexes are often solvatochromic, i.e., the colors of their solutions change remarkably according to the nature of the solvent. This study includes two main parts:

1) UV/Vis spectra in pure solvents.
2) UV/Vis spectra in binary solvent mixtures.

3.2.6.1 UV/Vis spectra of copper-MHQ complexes in pure solvents

The electronic absorption spectra of the present chelates in solution and as Nujol mulls were studied in the visible region. The visible absorption spectra of copper-MHQ complexes in different organic solvents (Fig. 4 & Table 4) show a broad band in the visible region that could be assigned to transfer of an electron to the $d_{x^2-y^2}$ orbital.[54]

A procedure used for the treatment of the experimental results in which the shift of the ν_{max} values of a series of copper–MHQ complexes measured in twelve pure solvents, (protic: MeOH, EtOH, 2-PrOH, n-BuOH and n-PenOH; and aprotic: DMF, DMSO, CHCl$_3$, Benzene, Me$_2$CO, 1,4-Diox, and EtAc) was first correlated with each one of the solvent parameters (AN, DN, π*, α, β, …etc)[55] individually to assess for reasonable explanation. Then, to provide an independent interpretation of the ν_{max} results in different pure solvents, the linear solvation energy relationship (LSER) method, based on Kamlet-Taft, multi-parameters has been performed using two, three or four solvent parameters for a given solvent. Finally, a conclusion was reached by taking into account only those parameters, which gave satisfactory in the linear regression. Good multi-parametric correlations were obtained when two solvent parameters were considered. The general relationship can be expressed by the following equation (1):

$$\nu_{max} = \nu^0_{max} + a\, X_1 + b\, X_2 + c\, X_3 + \text{---(1)}$$

Where, ν^0_{max} is the value of the ν_{max} in the virtual absence of solvent. X_1, X_2 and X_3 are different solvent parameters. a, b and c are coefficients of X_1, X_2 and X_3 which can be obtained by multiple linear regression analysis (MLRA).

The solvatochromic shift of the ν_{max} values for some of the current complexes as shown in Fig. 4 was correlated at first with polarity-polarizability (π*).

The correlations were found to be unsatisfactory (correlation coefficients, $r^2 \approx$ 3%). On the other hand, when the acidity scale (α) or the acceptor number (AN) of Mayer and Gutmann parameters, were correlated individually with the ν_{max} values, relatively good correlations ($r^2 \approx$ 90%) were obtained.

However, multi-parameter correlations were improved further ($r^2 \approx$ 98%). Correlations of ν_{max} with π* and α olvatochromic parameters of Kamlet and Taft were given in Table 5 with correlation coefficients (r^2) in the range 94.4 – 97.4.

The relative percentage influence of π^* and α on ν_{max} values was calculated directly from the π^* and α coefficients and was found to be in the range 40 - 13% and 60 - 87%, respectively. Another multi-parametric correlation was applied by involving the β parameter as an independent variable. However, the multiple correlation coefficient did not significantly differ from that obtained through the two parameters (π^* and α). This consequence suggests that the influence of β term on the ν_{max} values may be considered as negligible.

From the data given in Table 5, it can be deduced that the capability of copper-complexes to form hydrogen bond with proton donor solvents (as measured by the α term) plays an important role in determining ν_{max}. The positive sign of α coefficients (Table 5) indicates that, the hydrogen bond formed for the copper-complexes in protic solvents may stabilize the ground state rather than the excited state, resulting in hypsochromic shift. Moreover, the positive sign of π^* coefficient (except for complex **4**) as indicated in Table 5, suggests that the ground state is more polar than the excited state. This seems an entirely reasonable assumption, as the polarity–polarizability, π^* of the solvent increases the ground state becomes more stabilized than the excited state. This produces a hypsochromic shift of the absorption band (positive sign of the π^* coefficient).

Another good correlation was also found when the acceptor and donor numbers (AN and DN) of Gutmann, which measure the ability of solvent as an electron acceptor or electron donor; respectively were used as independent variables. The results obtained were collected in Table 5. These results demonstrate that, both solvent Lewis acidity (measured by the AN) and Lewis basicity (measured by the DN) are important to explain the observed variation in the ν_{max} values of the copper-complexes with the solvent nature, with a relative contributions 69.4-94.7% and 30.6-5.3% for AN and DN; respectively.

When dielectric constant (ε was included in the correlation, the correlation coefficients didn't significantly differ from that obtained when only DN and AN were only considered. These results suggest a negligible influence of ε term on the ν_{max} values except for complex **4^b**. This correlates well with the spectral data of the copper-complexes, if one assumes that the structure of the copper-MHQ complexes plays an important role in the d-d electronic transition responsible for the long-wavelength absorption band and its solvatochromic behavior.

Furthermore, the positive sign of AN coefficients indicates that the current copper-MHQ complexes are able to donate an electron pair to a solvent with high Lewis acidity. Therefore, Lewis acid–base interactions of the copper-MHQ complexes with the solvent molecules would also stabilize the ground state more than the excited state, resulting again in a hypsochromic shift of the d-d absorption band.

The main term that quantifies the Lewis acidity parameter (AN) of solvent is relatively important for copper complexes, as reflected from the magnitude of its coefficient, and its higher contribution percentage (Table 5). The positive sign of this coefficient indicates blue shift as the solvent's Lewis acidity increases. However, the effect of solvent's Lewis basicity term, DN is less significant as indicated from the low contribution percentage and/or the negative sign of its coefficient, leading to red shift as the donor strength of solvent increases. The former case might arises because, on one hand when a solvent exhibiting strong acceptor properties, it will decline the coordination of anion (preferentially solvating the anion), i.e., weaken the interaction between the anion and the central copper ion. On the other hand, the solvent accept the lone pair of electrons on the non-coordinated nitrogens, of MHQ ligand, i.e. act as electron-attracting centers. Consequently, the d-d absorption band shifted to a higher frequency as the solvent's acceptor property increases. However, in the latter case when the donor strength of the solvent increased, the solvent preferably coordinated the central metal ion forming an octahedral geometry, so the d-d band shifted to a lower frequency.

The quality of the fits obtained with the presented multi-parametric correlations for copper-complexes in the current study **1**, **2** and **4** are similar. On the basis of these results, it could be concluded that both the solvent electron accepting character (AN), or capability to donate a proton in a solute-solvent hydrogen bond donor (α), as well as the solvent polarity-polarizablity (π^*) properties are the most important factors necessary to explain the dependence of the shift of the ν_{max} values on the solvent nature. The relative contributions of these correlations suggest that, the shifts of the ν_{max} depend mainly on the AN and α parameters rather than π^* parameter.

Moreover, the relative contribution values given indicate generally, AN, α and π^* parameters are affected by the nature of the anion of the copper-complexes. Thus, the copper-complex which has chloride anion show a lower relative contribution

for AN parameter, chloride (69.4%) < perchlorate (79.8%) < nitrate (94.7%). This finding agrees well with the trend of relative contributions for π^* parameter: chloride (13.3%) < perchlorate (25.2%) < nitrate (40.1%). However, opposite trend was found in case of α parameter where: chloride (86.7%) > perchlorate (74.8%) > nitrate (59.5%).

3.2.6.2. UV/Vis spectra in binary solvent mixtures (preferential solvation studies on metal-MHQ complexes)

Solvent mixtures have become an important subject of research because of their frequent use and the wide field of application they offer.[56] The most important feature of these mixed solvents is the gradual variation of properties they show when their composition is gradually modified.

Therefore, it is currently considerable interest in the study of physicochemical phenomena in mixed solvent systems and their interpretation in terms of preferential solvation of solutes by one of the component solvents in the mixture.[57]
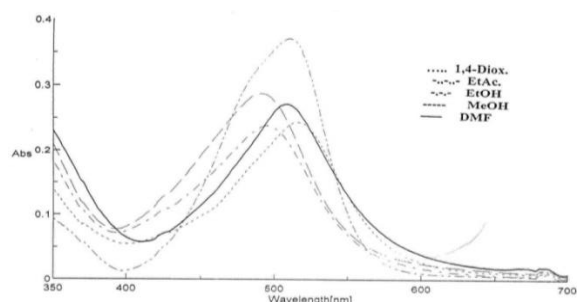

Fig. 4. Electronic absorption spectrum of $[Cu^{III}L(H_2O)].NO_3.MeOH(\,2)$ in different solvents at 25 °C.

The goal of this study is to monitor the effect of solute-solvent and solvent-solvent interactions on the preferential solvation characteristics. For this purpose, the d-d bands of complexes in binary solvent mixtures have been used as indicator solutes (Fig. 5).
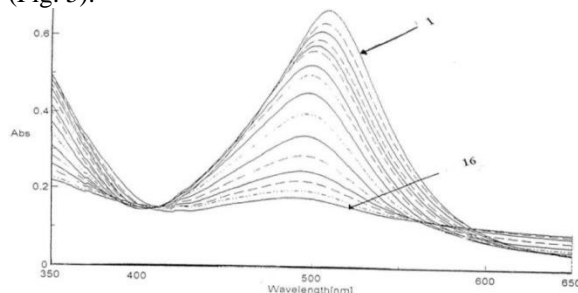

Fig. 5. Preferential solvation of $[Cu^{III}L(H_2O)].NO_3.MeOH(\mathbf{2})$ in DMF-H$_2$O solution at 25°C; the mole fraction of H$_2$O varied from X_{H2O} = 0 (1) - X_{H2O} = 0.70 (16).

Studying the solvatochromic and preferential solvation phenomenon of MHQ with Cu(II) metal ion for providing an insight into the microscopic characteristics of the cybotactic zone of solutes in mixed solvents. Table 6 gives the shift of the ν_{max} values of the current complexes measured in aqueous-DMF binary solvent mixtures (AB) at varied molar fractions of the component A (water).

Fig. 6 shows some representative examples of the ν_{max} values as a function of molar fractions of the component A in the bulk solution mixtures. The functional relationship of ν_{max} *vs.* X_A is non-linear for the most of the complexes under investigation. This is very similar to the partial vapor pressure with X_A plots for binary solvent mixtures. It is well established that the non-linearity of the ν_{max} *vs.* X_A plots arises due to preferential solvation of the present complexes which arises commonly, and because it modifies the neighborhood of the solute.[57]

Different criteria were used to assess the type and extent of the preferential solvation of the complexes in binary solvent mixtures, *viz.* the local molar fraction (X_A^L), excess function (ΔX), iso-solvation point (X_B^{iso}) and preferential solvation constant ($K_{A/B}$) parameters. Local molar fraction of the component solvents can be calculated as described earlier.[56a]

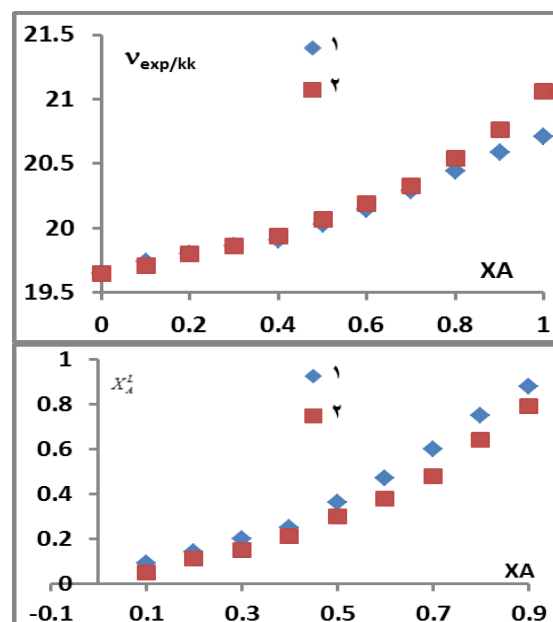**Fig. 6** Frequencies ($\nu_{exp/kk}$) of absorption bands of MHQ complexes (**1** & **2**) *vs.* X_{H2O} & local molar fractions (X_A^L) for the preferential solvation of these complexes *vs.* bulk molar fractions X_{H2O} of binary (H$_2$O-DMF) solvent at 25 °C.

Table 7 lists the calculated values of the local molar fractions (X_A^L). Fig. 6 shows the functional relationship of X_A^L vs. the bulk molar fractions (X_A), which is non-linear for all complexes in this study. The deviation from ideality, straight lines which represent the situation where local and bulk molar fractions are the same, indicating again to the specific interactions of the complex with the components of the solvent mixture.[53] The type and extent of deviation from the straight line, excess function (ΔX)

$$\Delta X = X_A^L - X_A$$

It may be taken as quantitative criteria of preferential solvation. The positive value of ΔX means the preference of component A (water) over the component B. The $\Sigma \Delta X$ values at all fractions could be used to quantify the extent of this preference, *vide infra*.

The iso-solvation point (X^{iso}), refers to the solvent composition in the bulk at which v_{max} of the complexes in the binary solvent mixture lies midway between those of v_{max} in pure solvent components. The calculated X_B^{iso} values for the present complexes in the binary mixtures are given in Table 8. The type and extent of preferential solvation could be also concluded from X_B^{iso} values. The negative deviation appears when X_B^{iso} < 0.5, and the positive deviation occurs when X_B^{iso} > 0.5, which indicates, the preference of component B (DMF) over the component A, in the former situation, and the opposite trend for the latter one.[56b]

Table 8 shows that, the values of X_B^{iso} < 0.5, for most complexes in water mixed with DMF, indicating preferential solvation by the component B (DMF).[56b] A more quantitative method to estimate the extent of preferential solvation of the complexes in binary solvent mixtures can be judged by the preferential solvation parameter $K_{A/B}$, using the thermodynamic model[56b] according to the following equation:

$$K_{A/B} = \frac{(Y_A / Y_B)_{local}}{(X_A / X_B)_{bulk}}$$ (2) where Y_A and Y_B represent local molar fractions of components A and B in the solvation shell and X_A and X_B refer to the same quantity in the bulk solvent. The parameter $K_{A/B}$ measures the tendency of the indicator complex to be solvated with the solvent A in

preference to the solvent B. According to equation mentioned above, the plot of (Y_A/Y_B) *vs* (X_A/X_B) will give straight line with slope $K_{A/B}$, which represent the preferential solvation constant. One can calculate $K_{A/B}$ using equation (2) and the calculated values are given in Table 8. These $K_{A/B}$ values concerning preferential solvation are the same as discussed above but they do allow a better inter-system comparison to be made. $K_{A/B} < 1$, means preference of component B (DMF) over component A (H_2O), in contrast $K_{A/B} > 1$ refers to the opposite trend. The conclusion given above can be extracted, for the studied complexes, from the data in Table 8. These data show that: $K_{A/B} < 1$ for most complexes. Specifying preferential solvation of the indicator complex by the component DMF in the former case and water in the latter case, respectively.

All possible combinations have been checked for the calculated preferential solvation parameters, $K_{A/B}$, $\Sigma \Delta X$ and X_B^{iso} given in Table 8 using multiple linear regression analysis. The best fits obtained, yield the following:

$$X_B^{iso} = 0.457 + 0.11 \ \Sigma \Delta X - 0.03 \ K_{A/B}$$
r = 0.98

The correlation coefficients value can be used to judge the agreement between the different criteria chosen in the present work. The agreement is very well, indicating the simplicity in the present system.

Table 8. Preferential solvation parameters of the MHQ complexes in binary of water (A)-DMF (B) solvent mixtures at 25 °C.

No.	$\Sigma \Delta v$	$\Sigma \Delta X$	X_A^{iso}	X_B^{iso}	$K_{A/B}$	dev. type
1	785.72	-0.77	0.64	0.36	0.48	-ve
2	2057.1	-1.39	0.72	0.28	0.39	-ve

The preferential solvation could be assigned to the net results of solvent-solvent and solute-solvent interactions. The former interaction might lead to form a new solvent species (S_{AB}) *via* donor-acceptor or hydrogen bonding interactions. This new solvent species can have properties, which are quiet different from those of pure solvents water (A) and DMF (B).[58] (Suggest the formation of S_{AB}, the ratio 1:1 molar fraction for solvents A and B was taken for the sake of simplicity). The co-solvent DMF which has a higher DN should interact with water, leading to decrease the extent of water cluster.

_____

3.2.7. Molecular modeling of the metal chelates of MHQ ligand

The heat of formation (Table 9) of the tautomeric form (I) is more positive than that of the tautomer (II), showing that the tautomer (I) is less stable than the other. The sulphate complex (**6**) has highest values of heat of formation, dipole moment, LUMO energy, HOMO energy and ΔE_{gap} than that the other complexes.

The best correlations between theoretical and experimental data (Table 9-10) obtained from *pm3* level, we can conclude the following remarks:

1) E_{HOMO} increases, as stability of complexes decreases and the length of the bonds (N19-O20 & N14-C15) decreases [complexes 1-3, 6].

2) The good correlation between length of C16-N19 and λ_{max} indicates that increasing of λ_{max} leads to decreasing stability of the complexes, thus the length of C16-N19 bonds decreases [complexes **3**, **6-8**].

Length of C16-N19 = 1.81 ($\pm$0.09151) - 0.00110 ($\pm$0.0002162) λ_{max} R-Sq = 92.8%
E_{HOMO} = 9.19 ($\pm$0.02113) - 11.0 ($\pm$0.0160) Length of N19-O20   R-Sq = 100.0%
E_{HOMO} = 15.7 ($\pm$0.3227) - 14.1 ($\pm$0.2311) Length of N14-C15   R-Sq = 99.9%

3) Values of energy gap (2.702-8.042 eV) indicate that the prepared compounds are potentially interesting electronic transitions as a result of their narrow energy gapes.[59]
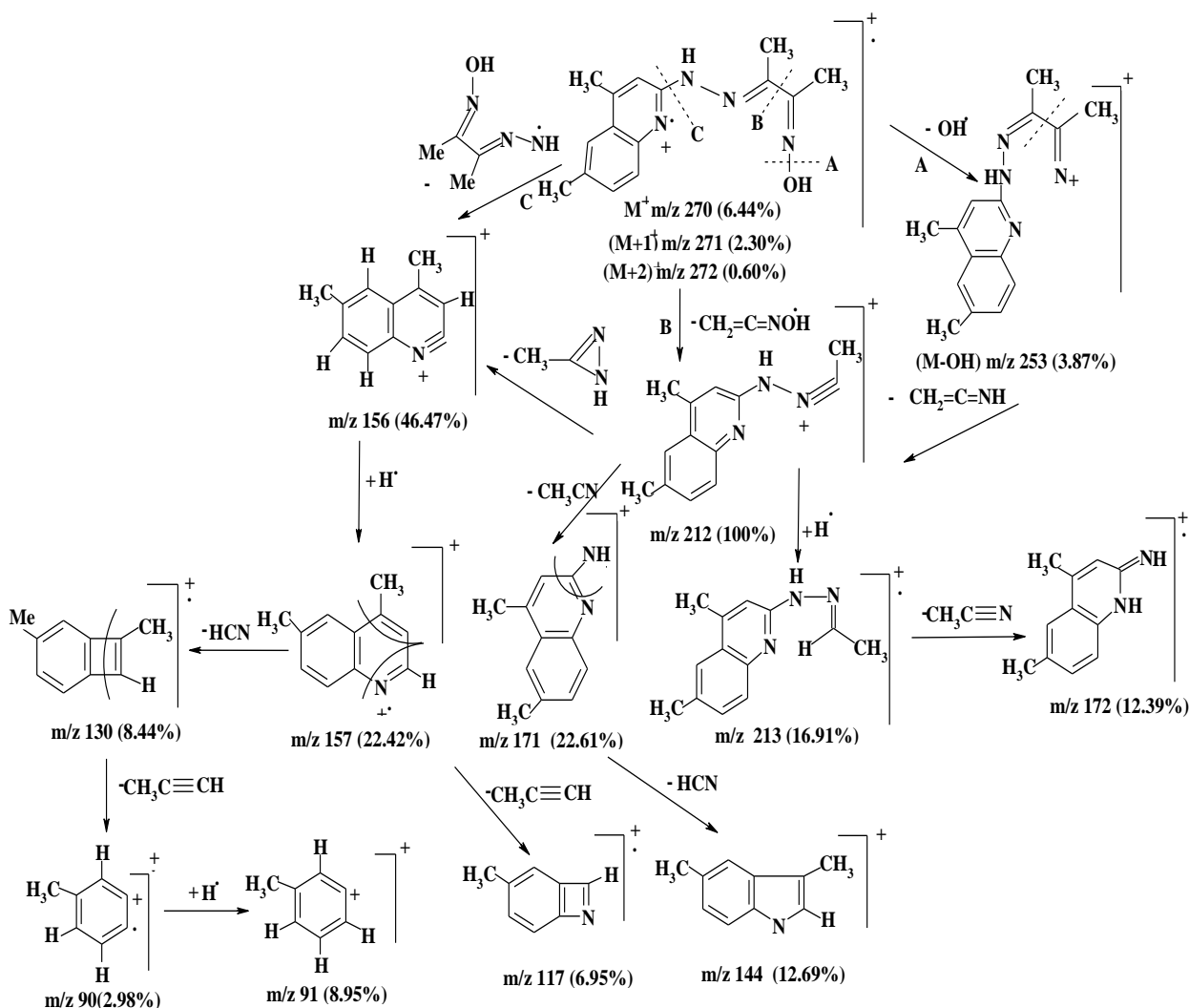
Scheme 3. Mass fragmentation patterns of MHQ ligand.

_____

Table 4. Electronic absorption spectral data of copper-MHQ complexes in different solvents.

No.	MeOH	EtOH	2-PrOH	ButOH	PenOH	DMF	DMSO	CHCl₃	Benzene	Me₂CO	1.4-Diox.	EtAc.
1	490	494	402	498	498	509	362	403	509	509	515	509
	324	326	324 Sh.	333	324 Sh.	345	311 Sh.	323	314 Sh.	306	336 Sh.	
2	491	496	404	498	500	509	364 Sh.	404	513	509	516	511
	325	235	330	330	324		308	328		312 Sh	328 Sh.	
4	490	402	402	402	399	510	504	522 Sh.	-----	400 Sh.	512	506
	325 Sh.	323 Sh.	324 Sh.	325 Sh.	326 Sh.	323 Sh.	367 Sh.	392 Sh.		332	328 Sh.	328 Sh.

Table 5a. Linear regression analysis (LRA) of the d–d transitions of Cu-MHQ complexes in different solvents *vs.* (AN, DN, ε, α, β and π*).

No.	AN			DN			ε			α			β			π*		
	$\nu^o_s/10^3$	AN	r^2	$\nu^o_s/10^3$	DN	r^2	$\nu^o_s/10^3$	ε	r^2	$\nu^o_s/10^3$	α	r^2	$\nu^o_s/10^3$	β	r^2	$\nu^o_s/10^3$	π*	r^2
1	19.34	23.5	91.0	19.37	22.6	46.4	19.58	14.2	30.5	19.59	805	94.8	19.31	1002	38.4	20.22	-648	4.8
2	19.27	24.4	94.8	19.26	25.5	57.8	19.50	16.4	39.1	19.53	802	94.1	19.19	1133	49	20.00	-384	1.7
4[a]	19.35	24.9	87.6	19.01	37	48.3	19.64	9.7	19.8	19.63	790	94.2	19.15	1258	24.5	20.20	-577	5.3
4[b]	25.35	-10.7	15.3	25.49	-19	84.7	25.63	-33.4	88.3	25.30	-485	39.6	25.51	-841	87.5	24.70	635	4.2

4[a] Cu – MHQ complex in MeOH, DMF, 1,4-Dioxane and EtAc. solvents.

Table 5b.Multilinear regression analysis (MLRA) of the d–d transitions of Cu-MHQ complexes in different solvents *vs* (Guttmann parameters; AN, DN and ε).

No.	$\nu^o_s/10^3$	ε		DN		r^2	$\nu^o_s/10^3$	ε		AN		r^2	$\nu^o_s/10^3$	DN		AN		r^2
		a	%	b	%			a	%	c	%			b	%	c	%	
1	19.37	1.9	8.5	20.5	91.5	46.6	19.34	0.03	0.1	23.5	99.9	91.0	19.38	-7.66	20.2	30.2	79.8	94.8
2	19.27	3.5	14	21.5	86	58.5	19.25	2.44	9.6	23.1	90.4	95.4	19.27	-1.48	5.3	26.7	94.7	95.6
4[a]	17.39	-51.8	24.7	158	75.3	100	19.38	-5.62	16.1	29.2	83.9	91.5	19.54	-13.4	30.6	30.4	69.4	89.6
4[b]	25.63	-20.2	67	-9.96	33	84.7	25.72	-32	88.3	-4.26	11.7	90.5	25.30	-25.4	67.2	12.4	32.8	95.7

4[a] Cu – MHQ complex in MeOH, DMF, 1,4-Dioxane and EtAc solvents.

Table 5c.Multilinear regression analysis (MLRA) of the d–d transitions of Cu-MHQ complexes in different solvents *vs.* (solvato parameters; α, β and π*).

No.	$\nu^o_s/10^3$	α		β		r^2	$\nu^o_s/10^3$	α		π*		r^2	$\nu^o_s/10^3$	β		π*		r^2
		$a/10^3$	%	$b/10^3$	%			$a/10^3$	%	$c/10^3$	%			$b/10^3$	%	$c/10^3$	%	
1	19.58	0.8	98	0.016	2	94.8	19.40	0.83	74.8	0.28	25.2	95.6	20.00	1.18	49	-1.23	51	54.4
2	19.44	3.5	14	0.24	86	95.4	19.16	0.85	59.5	0.57	40.1	97.4	19.76	1.28	55.9	-1.01	44.1	59.8
4[a]	19.62	0.78	95.7	0.035	4.3	94.2	19.71	0.78	86.7	-0.12	13.3	94.4	19.93	3.62	53.1	-3.2	46.9	99.6
4[b]	25.53	0.39	24.2	-1.22	75.8	95.3	27.46	-1.15	26.4	-3.2	73.6	72.4	26.37	-1.04	44.4	-1.3	55.6	100

4[a] Cu – MHQ complex in MeOH, DMF, 1,4-Dioxane and EtAc solvents.

_____

Table 5d. Multilinear regression analysis (MLRA) of the d–d transitions of Cu-MHQ complexes in different solvents *vs.* (AN, DN, ε, α, β andπ*).

No.	MLRA using Gutmann parameter, Eq.1								MLRA using solvato parameter, Eq.2							
	$v°_s/10^3$	ε		DN		AN		r^2	$v°_s/10^3$	α		β		π*		r^2
		a	%	b	%	C	%			A	%	b	%	c	%	
1	19.38	1.59	3.87	-9.33	22.69	30.2	73.44	95.00	19.37	897	59.76	-168	11.19	436	29.05	96.00
2	19.28	3.22	9.27	-4.90	14.11	26.60	76.61	96.20	19.16	852	59.92	-1.00	0.07	569	40.01	97.40
4[a]	17.50	-49.4	24.68	149	74.43	1.79	0.89	---	19.88	170	23.74	289	40.36	-257	35.89	---
4[b]	25.48	-14.2	38.06	-16.2	34.42	-6.91	18.52	---	26.45	-55.4	2.23	-1007	40.58	-1419	57.19	---

4[a] Cu – MHQ complex in MeOH, DMF, 1,4-Dioxane and EtAc solvents.

Table 6. Frequencies ($v_{exp/kk}$) of the absorption bands of MHQ complexes at various bulk molar fractions of solvent (X_A) at 25°C.

No.	Complex / X_{H2O}	0.00	0.10	0.20	0.30	0.40	0.50	0.60	0.70	0.80	0.90	1.00
1	$[Cu^{III}L(H_2O)]ClO_4$	19.65	19.74	19.80	19.86	19.91	20.03	20.14	20.29	20.44	20.59	20.71
2	$[Cu^{III}L(H_2O)]NO_3.MeOH$	19.65	19.71	19.80	19.86	19.94	20.07	20.19	20.33	20.54	20.76	21.06

Table 7. Local molar fractions (X_A^L) for the preferential solvation of MHQ complexes at *various* bulk molar fractions of binary (H₂O-DMF) solvent (X_A) at 25°C.

No.	Complex / X_{H2O}	0.10	0.20	0.30	0.40	0.50	0.60	0.70	0.80	0.90
1	$[Cu^{III}L(H_2O)]ClO_4$	0.09	0.14	0.20	0.25	0.36	0.47	0.60	0.75	0.88
2	$[Cu^{III}L(H_2O)]NO_3.MeOH$	0.05	0.11	0.15	0.21	0.30	0.38	0.48	0.64	0.79

Table 9. Structural parameters of the free H₂L ligand and its metal complexes.

No.	Property	Heat of Formation, kcal/mol	Dipole moment	HOMO Energy, [eV]	LUMO Energy, [eV]	ΔE_{gap}	ω	X	S	σ	η
	HL[a]	65.63036	3.335	-8.4174	-0.39295	8.024	2.418	4.405	0.125	0.249	4.012
	HL[b]	62.983695	2.219	-7.65578	-0.80163	6.854	2.609	4.229	0.146	0.292	3.427
1,2	$[Cu^{III}L(H_2O)]ClO_4$	-50.7681312	3.806	-4.240007	-0.55734	3.683	1.562	2.399	0.272	0.543	1.841
3	$[Cu^{III}L(MeOH)]Br$	-37.88395	3.546	-4.187561	0.65233	4.84	0.646	1.768	0.207	0.413	2.42
4	$[Cu_2^{II}(HL)Cl_3(H_2O)]$	-136.49411	10.38	-7.846422	-1.42088	6.426	3.341	4.634	0.156	0.311	3.213
5	$[Cu^{II}(HL)AcO(H_2O)_2]$	-231.209366	3.803	-3.482198	-0.78015	2.702	1.681	2.131	0.37	0.74	1.351
6	$[Cu_2^{II}(HL)_2SO_4(H_2O)_4].2½ H_2O$	-394.22900	17.47	-8.151398	-1.21327	6.938	3.16	4.682	0.144	0.288	3.469
7	$[Cu^{II}L(H_2O)]_2$	-155.11235	1.852	-7.72776	-0.52078	7.207	2.36	4.124	0.139	0.278	3.603
8	$[Cu_2^I(H_2L)I_2(MeOH)_2].MeOH$	-105.241386	4.413	-8.120422	-0.83964	7.281	2.757	4.48	0.137	0.275	3.64

L[a] tautomer (**I[a]**), L[b] tautomer (**II[b]**).

_____

Table 10. The selected bond lengths of optimized structures of the free H_2L ligand and its metal complexes.

Bond	Ligand				Complex					
	HL^a	HL^b	**(1)**	**(2)**	**(3)**	**(4)**	**(5)**	**(6)**	**(7)**	**(8)**
N19-O20	1.393	1.391	1.225		1.221	1.467	1.227	1.582	1.603	1.451
N19-C16	1.305	1.315	1.429		1.442	1.377	1.372	1.291	1.309	1.349
N14-C15	1.310	1.331	1.411		1.406	1.383	1.357	1.463	1.363	1.326
N7(Q)-C8	1.342	1.407	1.389		1.385	1.368	1.345	1.320	1.379	1.337
N7(Q)-M	----	----	----		1.909	----	----	----	----	----
O20-M	----	----	----		----	1.845	----	1.901	1.948	----
N19-M	----	----	1.863		1.889	----	1.881	-----	1.883	1.988
N14-M	----	----	1.885		1.894	1.899	1.903	2.069	1.915	1.949

HL^a tautomer (**I^a**), HL^b tautomer (**II^b**) and M = Cu.

Conclusions

Reaction of different Cu(II) salts NO_3^-, ClO_4^-, AcO^-, SO_4^{2-}, Cl^- and Br^- in addition to Cu^I as CuI. with 2-[α-(acetyloxime)ethylidenehydrazino]-4,6-dimethylquinoline (MHQ) yield mononuclear, binuclear and dimeric complexes. The structures of the prepared complexes have been characterized by elemental analysis and electronic, vibrational, electron, spin resonance and mass spectra. Multilinear regression analysis (MLRA) of the d–d transitions of Cu-MHQ complexes in different solvents *vs.* Guttmann parameters (AN, DN and ε) and solvato parameters (α, β and π*) have been determined. The structural optimizations of the ligand and its metal complexes have been performed by a *PM3* study by using the hyperchem program.

Conflicts of interest

"There are no conflicts to declare".

References

[1a] Yosef, H.A.A. and Ibrahim, N.M., Synthesis, Thermolysis, Photolysis and Antimicrobial Evaluation of some Novel Semicarbazones and Thiosemicarbazones Derived from 3-Methyl-benzothiazolinone Hydrazone, *Egypt. J. Chem.* 59(5) 867–885 (2016).

[1b] Xavier A.J., Thakur M., Marie J.M., Synthesis and spectral characterisation of hydrazone based 14-membered octaaza macrocyclic Ni (II) complexes. *J Chem Pharm Res.*; **4**, 986–90 (2012).

[1c] Koopaei M. N., Assarzadeh M. J., Almasirad A., Ghasemi-Nirib S. F., Amini M., Kebriaeezadeh A., et al, Synthesis and Analgesic Activity of NovelHydrazide and Hydrazine Derivatives, Iran J. Pharm. Res., 12(4), 721-722 (2013).

[1d] Kumar N., Chauhan L. S., Dashora N., Sharma C. S., Anticonvulant potential of Hydrazone derivatives: A Review., Sch. Acad. J. Pharm., 3 (5), 366-373 (2014).

[1e] Mohammad A. Anti-microbial potentials of hydrazonone derivatives: A promising scaffold. International Journal of Chemical and Applied Biological Sciences. Medknow; 1(1), 23 (2014).

[1f] Wang H, Ren S-X, He Z-Y, Wang D-L, Yan X-N, Feng J-T, et al. Synthesis, Antifungal Activities and Qualitative Structure Activity Relationship of Carabrone Hydrazone Derivatives as Potential Antifungal Agents. International Journal of Molecular Sciences [Internet]. MDPI AG; Mar 11; 15(3), 4257–72 (2014).

[2a] Abd El-Karim, S.S., Gouhar, R.S., Haiba, M.E., El-Zahar, M.I., Awad, G.E.A. and Bagato, O., Synthesis of Novel Derivatives Bearing Heterocycles-Tetrahydronaphthalene Conjugates for Antimicrobial and Antiviral Evaluation, Egypt. J. Chem. 57(4) 281-313 (2014).

[2b] Ibrahim N.M., Yosef H.A.A., Ewies E.F., Mahran M.R.H., Ali M.M., Mahmoud AE. Synthesis and Antitumor Evaluation of New Heterocycles Derived from 3-Methyl-2-benzothiazolinone Hydrazone. Journal of the Brazilian Chemical Society [Internet]. Sociedade Brasileira de Quimica (SBQ); 26(6), 1086-1097 (2015).

[2c] Potu°cˇkovaˊ E., Hrusˇkovaˊ K., Buresˇ J., KovarˇiˊkovaˊP., Sˇ pirkovaˊ I. A., Pravdiˊkovaˊ K., et al, Correction: Olfactory Performance Is Predicted by Individual Sex-Atypicality, but Not Sexual Orientation, PLoS ONE., 9(11), 1-17 (2014).

[2d] Sharma M., Chauhan K., Srivastava R.K., Singh S.V., Srivastava K., Saxena J.K., et al. Design and Synthesis of a New Class of 4-Aminoquinolinyl-and 9-Anilinoacridinyl Schiff Base Hydrazones as Potent Antimalarial Agents. Chemical Biology & Drug Design [Internet]. Wiley-Blackwell; Mar 13; 84(2), 175–81 (2014).

[2e] Asif M., Anti-microbial potentials of hydrazonone derivatives: A promising scaffold. International Journal of Chemical and Applied Biological Sciences., Int. J. Adv. Chem., 2(2), 85-103 (2014).

[3a] Zaki, M.Y., Cytotoxicity of Novel Hydrazide-hydrazone Derivatives towards Tumor and Normal Cell Lines, Egypt. J. Chem. 56(1) 25-34 (2013).

[3b] Khattab T.A., Haggag K.M., Elnagdi M.H., Abdelrahman A.A. and Aly S.A., Microwaveassisted synthesis of arylazoaminopyrazoles as disperse dyes for textile printing. Zeitschrift für Anorganische und Allgemeine Chemie, 642 (13), 766-772 (2016).

[3c] Khattab T.A., Elnagdi M.H., Haggaga K.M., Abdelrahmana A.A. and Aly S.A., Green synthesis, printing performance, and antibacterial activity of disperse dyes incorporating arylazopyrazolopyrimidines. AATCC Journal of Research, 4 (4), 1-8 (2017).

[3d] Khattab T.A. and Gaffer H.E., Synthesis and application of novel tricyanofuran hydrazone dyes as sensors for detection of microbes. Coloration Technology; 132 (6), 460-465 (2016).

[3e] Al-Sehemi A.G., Irfan A., Asiri M. and Ammar Y.A., Molecular design of new hydrazone dyes for dye-sensitized solar cells: Synthesis, characterization and DFT study. Journal of Molecular Structure; 1019, 130-134 (2012).

[3f] Khattab T.A., Tiu B.D.B., Adas S., Bunge S.D. and Advincula R.C., pH triggered smart organogel from DCDHF-Hydrazone molecular switch. Dyes and Pigments, 130, 327-336 (2016).

[3g] Rollas S. and Kucukguzel S.G., Biological activities of hydrazone derivatives. Molecules, 12 (8), 1910-1939 (2007).

[3h] Ezz El-Arab E., El-Said A.I., Amine M.S. and Moharram H.H., Synthesis and Antitumor Activity Evaluation of New 2-(4-aminophenyl) benzothiazole/ oxazole/imidazole Derivatives. Egyptian Journal of Chemistry, 59 (6), 967-984 (2016).

[4a] Samy, F. and Taha, A., Synthesis, Spectroscopic, Biological and Theoretical Studies of Nano Complexes Derived from TriazineHydrazone, Egypt. J. Chem.,61(5), 731-746 (2018).

[4b] Samy, F., Taha, A., Seleem, H.S. and Ramadan, A.A.T., pH-Metric Studies of (2-pyrrole)-(5,6-diphenyl-[1,2,4]-triazin-3-yl)hydrazone with Inner Transition Metals, Egypt. J. Chem. 63(11), 4243-4252 (2020).

[4c] El-Saied F.A., Al-Hakimi A.N. and Wahba M.A., Preparation, Characterization and Antimicrobial Activities of N'-((3-(hydroxyimino) butan-2- ylidene)-2 (phenylamino) acetohydrazide and Its Metal Complexes. Egyptian Journal of Chemistry; 60 (1), 1-24 (2017).

[4d] EL-Sayed N.S., El-Ziaty A.K., El-Meligy M.G. and Nagieb A.Z., Syntheses of New Antimicrobial Cellulose Materials Based 2-((2-aminoethyl) amino)-4-aryl-6-indolylnicotinonitriles. Egyptian Journal of Chemistry, 60 (3), 465-477 (2017).

[4e] Misra R.N., Kimball S.D., Rawlins D.B., Webster K.R. and Bursuker I., Use of pyrazolo[3, 4-b] pyridine as cyclin dependent kinase inhibitors. U.S. Patent, 6,107, 305 (2000).

[4f] Suvarapu L.N., Seo Y.K., Baek S.-O. and Ammireddy V.R., Review on analytical and biological applications of hydrazones and their metal complexes. Journal of Chemistry, 9 (3), 1288-1304 (2012)

[5a] Shebl, M., Coordination behavior of new bis(tridentate ONO, ONS and ONN) donor hydrazones towards some transition metal ions: Synthesis, spectral, thermal, antimicrobial and antitumor studies, J. Mol. Struct.,1128, 79-93 (2017).

[5b] Shebl, M., Saleh, A.A., Khalil, S.M.E., Dawy, M. and Ali, A.A.M., Synthesis, spectral, magnetic, DFT calculations, antimicrobial studies and phenoxazinone synthase biomimetic catalytic activity of new binary and ternary Cu(II), Ni(II) and Co(II) complexes of a tridentate ONO hydrazone ligand, Inorganic and Nano-Metal Chemistry, 51, 195-209 (2021).

[5c] Loncle, C., Brunel, J.M., Vidal, N., Dherbomez, M. and Letourneux, Y., Synthesis and antifungal activity of cholesterol-hydrazone derivatives. Eur. J. Med. Chem. 39, 1067 (2004).

[5d] Papakonstantinou-Garoufalias, S., Pouli, N., Marakos, P. and Chytyroglou-Ladas, A., Synthesis antimicrobial and antifungal activity of some new 3 substituted derivatives of 4-(2,4-dichlorophenyl)-5-adamantyl-1H-1,2,4-triazole. Farmaco, 57, 973 (2002).

[5e] Vicini, P., Zani, F., Cozzini, P. and Doytchinova, I., Hydrazones of 1,2-benzisothiazole hydrazides: synthesis, antimicrobial activity and QSAR investigations. Eur. J. Med. Chem. 37, 553 (2002).

[5f] Kaushik, D., Khan, S. A., Chawla, G. and Kumar, S., N'-[(5-chloro-3-methyl-1-phenyl-1 H-pyrazol-4-yl) methylene] 2/4-substituted hydrazides: Synthesis and anticonvulsant activity. Eur. J. Med. Chem. 45, 3943 (2010).

[5g] Sridhar, S.K., Pandeya, S.N., Stables, J.P. and Atmakuru, R., Anticonvulsant activity of hydrazones, Schiff and Mannich bases of isatin derivatives. Eur. J. Pharm. Sci. 16, 129 (2002).

[5h] Küçükgüzel, S.G., Mazi, A., Sahin, F., Öztürk, S. and Stables, J.P., Synthesis and biological activities of diflunisal hydrazide-hydrazones. Eur. J. Med. Chem. 38, 1005 (2003).

[6a] Shebl, M. and Khalil, S.M.E., Synthesis, spectral, X-ray diffraction, antimicrobial studies, and DNA binding properties of binary and ternary complexes of pentadentate N2O3carbohydrazone ligands, MonatshChem, 146, 15–33 (2015).

[6b] Todeschini, A.R., Küçükgüzel, S.G., Mazi, A., Sahin, F., Öztürk, S. and Stables, J.,

Synthesis and biological activities of diflunisal hydrazide–hydrazones. Eur. J. Med. Chem. 38, 1005 (2003).

[6c] Gaston, M.A., Dias, L.R.S., Freitas, A.C.C., Miranda, A.L.P. and Barreiro, E.J., Synthesis and analgesic properties of new 4-arylhydrazone 1-H pyrazole [3,4-b] pyridine derivatives. Pharmac. Acta Helvet. 71, 213 (1996).

[6d] Melnyk, P., Leroux, V., Sergheraert, C. and Grellier, P., Design, synthesis and in vitro antimalarial activity of an acylhydrazone library. Bioorg. Med. Chem. Lett. 16, 31(2006).

[6e] Bedia, K.K., Elçin, O., Seda, U., Fatma, K., Nathaly, S., Sevim, R. and Dimoglo, A., Synthesis and characterization of novel hydrazide–hydrazones and the study of their structure–antituberculosis activity. Eur. J. Med. Chem. 41, 1253 (2006).

[6f] Vavříková, E., Polanc, S., Kočevar, M., Horváti, K., Bősze, S., Stolaříková, J., Vávrová, K. and Vinšová, J., New fluorine-containing hydrazones active against MDR-tuberculosis. Eur. J. Med. Chem. 46, 4937 (2011).

[7a] Samy, F., Taha, A. and Omar, F.M., New solvatochromic complexes of 1,2-bis[(5,6-diphenyl-1,2,4-triazin3-yl)hydrazinylidene-methy]benzene: Synthesis, spectroscopic, biological, docking and theoretical studies, Appl. Organometal. Chem. e6375, (2021).

[7b] Samy, F. and Omar, F.M., Synthesis, characterization, antitumor activity, molecular modeling and docking of new ligand, (2,5-pyrrole)-bis(5,6-diphenyl-[1,2,4]-triazin-3-yl)hydrazone and its complexes, J. Mol. Struct.1222, 128910 (2020).

[7c] Omar, F.M. and Samy, F., Synthesis, spectral, thermal, potentiometric, antitumor, antimicrobial and PM3 studies of pyridazinonehydrazone metal complexes, J. Mol. Struct.1242, 130744 (2021).

[7d] Shebl, M., Khalil, S.M.E., Kishk, M.A.A., El-Mekkawi, D.M. and Saif, M., New less toxic zeolite-encapsulated Cu(II) complex nanomaterial for dual applications in biomedical field and wastewater remediation, Appl. Organometal. Chem. 33, e5147 (2019).

[7e] Patole, J., Sandbhor, U., Padhye, S., Deobagkar, D.N., Anson, C.E. and Powell, A., Structural chemistry and In vitro antitubercular activity of acetylpyridine benzoyl hydrazone and its copper complex against Mycobacterium smegmatis. Bioorg. Med. Chem. Lett. 13, 51 (2003).

[7f] Maccari, R., Ottanà, R. and Vigorita, M.G., Part 14, In vitro advanced antimycobacterial screening of isoniazid-related hydrazones, hydrazides and cyanoboranes. Bioorg. Med. Chem. Lett. 15, 2509 (2005).

[8] El-Taweel, F.M.A., Elaamey, A.A. and Elmougy, Sh.M.,Studies on Substituted Heteroarenes: New Synthesis of Substituted Pyrrole, Pyridine, Pyrazolo[4,3-bpyridine, Pyrano [3,2-c]quinoline, Benzo [f] chromene, Benzo[h] chromene, Chromeno [8,7-h]chromene, Chromeno[6,5-f] chromene and 2H-chromene Derivatives, Egypt. J. Chem., 54(6), 703-721 (2011).

[9] Thangaraja, M., Gengana, R.M., Ranjanb, B. and Muthusamyc,R., Synthesis, molecular docking, antimicrobial, antioxidant and toxicity assessment of quinoline peptides,J. Photochem. &Photobio., B: Bio.,178, 287-295 (2018).

[10] Hu, Y., Gao, C., Zhang, S., Xu, L., Xu, Z., Feng, L., Wu, X. and Zhao, F., Quinoline hybrids and their antiplasmodial and antimalarial activities, Eur. J. Med. Chem.,139, 22-47 (2017).

[11] Mandewale, M.C., Thorat, B., Nivid, Y., Jadhav, R., Nagarsekar, A. and Yamgar, R.,Synthesis, structural studies and antituberculosis evaluation of new hydrazone derivatives of quinoline and their Zn(II) complexes,J. Saudi Chem. Soc., 22, 218-228 (2018).

[12] Sureshkumar, K., Maheshwaran, V., Rao, T.D. , Themmila, K., Ponnuswamy, M.N., Kadhirvel, S. and Dhandayutham, S., Synthesis, characterization, crystal structure, in-vitro anti-inflammatory and molecular docking studies of 5-mercapto-1-substituted tetrazole incorporated quinoline derivative, J. Mol. Struct., 1146, 314-323 (2017).

[13] Thirunavukkarasu, T., Sparkes, H.A. and Natarajan, K., Quinoline based Pd(II) complexes: Synthesis, characterization and evaluation of DNA/protein binding, molecular docking and in vitro anticancer activity, Inorg. Chim.Acta, 482, 229-239 (2018).

[14] Seleem, H.S., El-Inany, G.A., Eid, M.F., Mousa, M.A. and Hanafy, F.I., Complexation of some Hydrazones Bearing the Quinoline Ring. Potentiometric Studies, J. Braz. Chem. Soc., 17, 723-729 (2006).

[15] Seleem, H.S., El-Inany, G.A., Mousa, M.A. and Hanafy, F.I., Spectroscopic studies on 2-[2-(4-methylquinolin-2-yl)hydrazono]-1,2-diphenylethanone molecule and its metal complexes, Spectrochim. Acta A, 74(4), 869-874 (2009).

[16] Seleem, H.S., El-Inany, G.A.,Mousa, M.A.and Hanafy, F.I.,Spectroscopic and pH-metric studies of the complexation of 3-[2-(4-methylquinolin-2-yl)hydrazono]butan-2-one oxime compound, Spectrochim. Acta A, 75, 1446–1451 (2010).

[17] Pavan, F.R., Maia, P.I.S., Leite, S.R.A., Deflon, V.M., Batista, A.A., Sato, D.N., Franzblau, S.G. and Leite, C.Q.F., Thiosemicarbazones, semicarbazones, dithiocarbazates and hydrazide/hydrazones: Anti – Mycobacterium tuberculosis activity and cytotoxicity. Eur. J. Med. Chem. 45, 1898-1905 (2010).

[18] Karalı, N., Kocabalkanlı, A., Gürsoy, A. and Ateş, Ö., Synthesis and antitubercular activity of 4-(3-coumarinyl)-3-cyclohexyl-4-thiazolin-2-one benzylidenehydrazones. Farmaco, 57, 589-93 (2002).

[19] Seleem, H.S., El-Inany, G.A., El-Shetary, B.A., Mousa, M.A. and Hanafy, F.I., The ligational behavior of an isatinicquinolylhydrazone towards copper(II)- ions, Chem. Central J., 5(20), (2011).

[20] Seleem, H.S., Transition metal complexes of an isatinicquinolylhydrazone, Chem. Central J., 5(35), (2011).

[21] Seleem, H.S.and Mousa, M.A., Ligand substitution reactions of a phenolic quinolylhydrazone; oxidovanadium (IV) complexes, Chem. Central J.,5(47), (2011).

[22a] Samy, F., Seleem, H.S., Taha, A., Shebl, M. and Hanafy, F.I., pH-metric and theoretical studies of the complexation of 2-[α-(o-hydroxyphenyl) ethylidenehydrazino]-4,6-dimethylquinoline and 2-[α-(o-

_____

methoxyphenyl)methylidenehydrazino]-4,6-dimethylquinoline, Egypt. J. Chem. 62(4), 691-705 (2019).

[22b] El-Shafiy, H.F. and Shebl, M., Oxovanadium(IV), cerium(III), thorium(IV) and dioxouranium(VI) complexes of 1-ethyl-4-hydroxy-3-(nitroacetyl)quinolin-2(1H)-one: Synthesis, spectral, thermal, fluorescence, DFT calculations, antimicrobial and antitumor studies, J. Mol. Struct., 1156, 403-417 (2018).

[23a] Das, L.K., Biswas, A., Kinyon, J.S., Dalal, N.S., Zhou, H. and Ghosh, A., Di-, Tri-, and Tetranuclear Nickel(II) Complexes with Oximato Bridges: Magnetism and Catecholase-like Activity of Two Tetranuclear Complexes Possessing Rhombic Topology, Inorg. Chem.,52(20), 11744–11757 (2013).

[23b] Koumousi, E.S., Raptopoulou, C.P., Perlepes, S.P., Escuer, A. and Stamatatos T.C., Strong antiferromagnetic coupling in doubly N,O oximato-bridged dinuclear copper(II) complexes, Polyhedron, 29, 204–211 (2010).

[24a] Costes, J. andVendier, L., Cu—Ln complexes with a single μ-oximato bridge, ComptesRendusChim., 13(6–7), 661-667 (2010).

[24b] Samy, F. and Shebl, M., Synthesis, spectroscopic, biological, and theoretical studies of new complexes from (E)-3-(2-(5, 6- diphenyl-1,2,4- triazin-3-yl)hydrazono)butan-2-one oxime, Appl. Organometal. Chem. 34, e5502 (2020).

[25] Adly, O.M.I., Shebl, M., Abdelrahaman, E.M. and El-Shetary, B.A., Synthesis, spectroscopic, X-ray diffraction, antimicrobial and antitumor studies of Ni(II) and Co(II) complexes derived from 4-acetyl-5,6-diphenyl-3(2H)-pyridazinone and ethylenediamine, J. Mol. Struct.,1219, 128607 (2020).

[26a] Seleem, H.S., El-Shetary, B.A., Khalil, S.M.E., Mostafa, M. and Shebl, M., Structural diversity in copper(II) complexes of bis(thiosemicarbazone) and bis(semicarbazone) ligands, J. Coord. Chem.,58(6), 479-493 (2005).

[26b] Shebl, M., Adly, O.M.I., Taha, A. and Elabd, N.N., Structural variety in copper(II)

complexes of 3-formylchromone: Synthesis, spectral, thermal, molecular modeling and biological Studies, J. Mol. Struct., 1147, 438-451 (2017).

[27a] Shebl, M., Ibrahim, M.A., Khalil, S.M.E., Stefan, S.L. and Habib, H., Binary and ternary copper(II) complexes of a tridentate ONS ligand derived from 2-aminochromone-3 carboxaldehyde and thiosemicarbazide: Synthesis, spectral studies and antimicrobial activity, Spectrochim. Acta A,115, 399–408 (2013).

[27b] Shebl, M., Khalil, S.M.E., Taha, A. and Mahdi, M.A.N., Synthesis, spectroscopic studies, molecular modeling and antimicrobial activity of binuclear Co(II) and Cu(II) complexes of 4,6-diacetylresorcinol, Spectrochim. Acta A,113, 356–366 (2013).

[27c] Taha, A., Adly, O.M.I. and Shebl, M., Reactivity and molecular modeling of new solvatochromic mixed-ligand copper(II) chelates of 2-acetylbutyrolactone and dinitrogen bases, Spectrochim. Acta A,140, 74–84 (2015).

[28a] Shebl, M., Adly, O.M.I., Abdelrhman, E.M. and El-Shetary, B.A., Binary and ternary copper(II) complexes of a new Schiff base ligand derived from 4-acetyl-5,6-diphenyl-3(2H)-pyridazinone: Synthesis, spectral, thermal, antimicrobial and antitumor studies, J. Mol. Struct.,1145, 329-338 (2017).

[28b] Abdelrhman, E.M. El-Shetary, B.A., Shebl, M., Adly, O.M.I.,Coordinating behavior of hydrazone ligand bearing chromone moiety towards Cu(II) ions: Synthesis, spectral, density functional theory (DFT) calculations, antitumor, and docking studies,Appl. Organometal. Chem.,35, e6183 (2021).

[28c] Shebl, M., Synthesis and spectroscopic studies of binuclear metal complexes of a tetradentate N2O2 Schiff base ligand derived from 4,6-diacetylresorcinol and benzylamine, Spectrochim. Acta A,70, 850-859 (2008).

[28d] Shebl, M., El-ghamry, M.A., Khalil, S.M.E. and Kishk, M.A.A., Mono- and binuclear copper(II) complexes of new hydrazone ligands derived from 4,6-diacetylresorcinol: Synthesis, spectral studies and antimicrobial activity, Spectrochim. Acta A,126, 232–241 (2014).

_____

[29] Seleem, H.S., El-Shetary, B.A., Khalil, S.M.E. and Shebl, M., Potentiometric and spectrophotometric studies of the complexation of Schiff-base hydrazones containing the pyrimidine moiety, J. Serb. Chem. Soc., 68, 729-748 (2003).

[30a] Seleem, H.S., Ramadan, A.A.T., Taha, A., Eid, M.F. and Samy, F., The complexation of a novel squaricbis(thiosemicarbazone); 3,4-bis{[(aminothioxomethyl)-amino]azamethylene}cyclobut-ene-1,2-diol, Spectrochim. Acta A, 78(3), 1097-1104 (2011).

[30b] Samy, F., Ramadan, A.A.T., Taha, A. and Seleem., H.S., Cobalt(II) and Nickel(II) complexes of hydrazone ligand ({(1E)-1-Aza-2-pyrrol-2-ylvinyl}{5,6-diphenyl(1,2,4-triazin-3-yl)}amine): Synthesis, spectral, pH-metric, antimicrobial and PM3 studies, Asian J. Chem.,. 28(12), 2650-2660 (2016).

[30c] Shebl, M., Synthesis, spectral and magnetic studies of mono- and bi-nuclear metal complexes of a new bis(tridentate NO2) Schiff base ligand derived from 4,6-diacetylresorcinol and ethanolamine, Spectrochim. Acta A,73, 313–323 (2009).

[30d] Shebl, M.,Khalil, S.M.E. and Al-Gohani, F.S., Preparation, spectral characterization and antimicrobial activity of binary and ternary Fe(III), Co(II), Ni(II), Cu(II), Zn(II), Ce(III) and UO2(VI) complexes of a thiocarbohydrazone ligand, J. Mol. Struct., 980, 78-87 (2010).

[30e] Shebl, M., Khalil, S.M.E., Ahmed, S.A. and Medien, H.A.A., Synthesis, spectroscopic characterization and antimicrobial activity of mono-, bi- and tri-nuclear metal complexes of a new Schiff base ligand, J. Mol. Struct., 980, 39-50 (2010).

[30f] Adly, O.M.I., El-Shafiy, H.F. and Shebl, M., Synthesis, spectroscopic studies, DFT calculations, antimicrobial and antitumor activity of tridentate NNO Schiff base metal complexes based on 5-acetyl-4-hydroxy-2H-1,3-thiazine-2,6(3H)-dione, J. Mol. Struct., 1196, 805-818 (2019).

[31] Taha, A., Farag, A.A.M., Adly, O.M.I., Roushdy , N., Shebl, M. and Ahmed, H.M. , Synthesis, spectroscopic, DFT and optoelectronic studies of 2-benzylidene-3-hydroxy -1-(5,6-diphenyl-1,2,4-triazine-3-yl)hydrazine metal complexes, J. Mol. Struct., 1139, 31-42 (2017).

[32a] Khalil, S.M.E., Shebl, M. and Al-Gohani, F.S., Zinc(II) Thiosemicarbazone Complex As a Ligand Towards Some Transition Metal Ions: Synthesis, Spectroscopic and Antimicrobial Studies, ActaChim. Slov.,57, 716-725 (2010).

[32b] S. M. E. Khalil, H. S. Seleem, B. A. El-Shetary, M. Shebl, Mono- and Bi-Nuclear Metal Complexes of Schiff-Base Hydrazone (ONN) Derived from o-Hydroxyacetophenone and 2-Amino-4-Hydrazino-6-Methyl Pyrimidine, J. Coord. Chem., 55, 883-899 (2002).

[33] Shebl, M., Mononuclear, homo- and hetero-binuclear complexes of 1-(5-(1-(2-aminophenylimino)ethyl)-2,4-dihydroxyphenyl)ethanone: synthesis, magnetic, spectral, antimicrobial, antioxidant, and antitumor studies, J. Coord. Chem.,69(2), 199–214 (2016).

[34] Fetoh, A., El-Gammal, O.A., Abu El-Reash, G.M.,Antioxidant and antitumor activities of Cr(III), Mn(II), Fe(III), Cd(II),Zn(II) and Hg(II) complexes containing a carbohydrazone ligandending by 4-pyridyl ring, J. Mol. Struct., 1173, 100-110 (2018).

[35a] Shebl, M., Adly, O.M.I., El-Shafiy, H.F., Khalil, S.M.E., Taha, A. and Mahdi, M.A.N.,Structural variety of mono- and binuclear transition metal complexes of 3-[(2-hydroxy-benzylidene)-hydrazono]-1-(2-hydroxyphenyl)-butan-1-one: Synthesis, spectral, thermal, molecular modeling, antimicrobial and antitumor studies, J. Mol. Struct., 1134, 649-660 (2017).

[35b] Shebl, M., Synthesis, spectroscopic characterization and antimicrobial activity of binuclear metal complexes of a new asymmetrical Schiff base ligand: DNA binding affinity of copper(II) complexes, Spectrochim. Acta A,117, 127-137 (2014).

[36a] Shebl, M., Saif, M., Nabeel, A.I. and Shokry, R.,New non-toxic transition metal nanocomplexes and Zn complex-silicaxerogelnanohybrid: Synthesis, spectral studies, antibacterial, andantitumor activities, J. Mol. Struct.,1118, 335-343(2016).

[36b] Seleem, H.S., El-Shetary,B.A. and Shebl, M., Synthesis and characterization of a novel

_____

series of metallothiocarbohydrazone polymers and their adducts, Heteroatom Chem., 18, 100-107 (2007).

[36c] El-Shafiy, H.F. and Shebl, M., Binuclear oxovanadium(IV), cerium(III) and dioxouranium(VI) nano complexes of a bis(bidentate) ligand: Synthesis, spectroscopic, thermal, DFT calculations and biological studies, J. Mol. Struct., 1194, 187-203 (2019).

[36d] Taha, A., Farag, A.A.M., Shebl, M., Ammar, A.H. and Ahmed, H.M. Synthesis, molecular orbital, optical and device characterization of mononuclear mixed ligand nickel(II) complex of phthalate with N,N,N`,N`-tetramethylethylene- diamine for photodiode applications, Spectrochim. Acta A,152, 218-225 (2016).

[37a]Adly, O.M.I., Shebl, M., El-Shafiy, H.F., Khalil, S.M.E., Taha, A. and Mahdi, M.A.N., Synthesis, spectroscopic characterization, antimicrobial and antitumor studies of mono-, bi- and tri-nuclear metal complexes of a new Schiff base ligand derived from o-acetoacetylphenol, J. Mol. Struct., 1150, 507-522 (2017).

[37b] Shebl, M., Seleem, H.S. andEl-Shetary, B.A.Ligational behavior of thiosemicarbazone, semicarbazone and thiocarbohydrazone ligands towards VO(IV), Ce(III), Th(IV) and UO2(VI) ions: Synthesis, structural characterization and biological studies, Spectrochim. Acta A,75(1), 428-436(2010).

[37c] Shebl, M., Khalil, S.M.E., Taha, A. and Mahdi, M.A.N., Structural diversity in binuclear complexes of alkaline earth metal ions with 4,6-diacetylresorcinol, J. Mol. Struct.,1027, 140-149(2012).

[38] Adly, O.M.I., Taha, A. and Fahmy, S.A., Synthesis, spectral characterization, molecular modeling and antimicrobial activity of new potentially N2O2 Schiff base complexes, J. Mol. Struct.,1054–1055, 239-250 (2013).

[39] Seleem, H.S., Emara, A.A. and Shebl, M., The relationship between ligand structures and their CoII and NiII complexes: Synthesis and characterization of novel dimeric CoII/CoIII complexes of

bis(thiosemicarbazone), J. Coord. Chem.,58(12), 1003-1019 (2005).

[40] Ismail, T.M., Mononuclear and binuclear Co(II), Ni(II), Cu(II), Zn(II) and Cd(II) complexes of Schiff-base ligands derived from 7-formyl-8-hydroxyquinoline and diaminonaphthalenes, J. Coord. Chem.,58, 141-151 (2005).

[41] Jones, C.J., "d- and f- Block Chemistry" Polestar Wheatons Ltd, Exeter (2001).

[42] Mackay, K.M. and Mackay, R.A. "Modern Inorganic Chemistry" 3rd End; Thomson Litho Ltd (Scotland) (1981).

[43] Iskander, M.F., Khalil, T.E., Haase, W., Foro, S., and Lindner, H.J., Synthesis, characterization and magnetochemical studies of some imidazole and imidazolate copper (II) complexes derived from N-salicylideneacetylhydrazine: X-ray crystal and molecular structures of [imidazole(N-Salicylideneacetylhydrazinato)ONO'(-2)] Copper(II) and Potassium [Mono((μ-imidazolate)bis(N-Salicylideneacetylhydrazinato] dicopper(II),J. Coord. Chem.,58(2), 111-123 (2005).

[44] Iskander, M.F., El-Sayed, L., Salem, N., Werner, R. and Haase, W., Synthesis, characterization and magnetochemical studies of dicopper(II) complexes derived from bis(N-salicylidene)-dicarboxylic acid dihydrazides,J. Coord. Chem.,58, 125-139 (2005).

[45]**Shebl**, M., Synthesis, spectral studies, and antimicrobial activity of binary and ternary Cu(II), Ni(II), and Fe(III) complexes of new hexadentate Schiff bases derived from 4,6-diacetylresorcinol and amino acids., *J. Coord. Chem.,*62(19), 3217-3231(2009).

[46] El-Tayeb, M.A. and Sulfab, Y.,Synthesis and characterization of silver(III) complexes with tetradentate and tridentate ligands with imine-oxime groups, Polyhedron, 26(1), 39-42(2006).

[47] Sulfab, Y. and Al-Sogair, F.M., Stabilization of the trivalent oxidation state of copper by tetradentate imine–oxime ligands, Transition Met. Chem.,27, 299-306 (2002).

[48] Mousa, M., M. Sc. Teacher's Preparation Thesis, Faculty of Education, Ain Shams University, Egypt (2005).

[49] I. C. Nag and A. Chakravorty, Monovalent, trivalent and tetravalent nickel, Coord. Chem. Rev., 33(2), 87-147 (1980).

[50] Margerum, D. and Owens, G., Copper (III) complexes and their reactions, Metal Ions in Biological Systems,12, 75 (1981).

[51] Hamilton, G.A., J. Am. Chem. Soc.,100, 1899-1912 (1978).

[52] Knof, U., Weyhermüller, T., Wolter, T. andWiegbardt, K., Synthesis of low spin [MnII(L2)2]I2·2MeOH and [CuIII(L1)] *via* condensation of *S*-methylisothiosemicarbazide and pentane-2,4-dione in the presence of air, J. Chem. Soc. Chem. Comm., 726-728 (1993).

[53] Halperin, W.P., Quantum size effects in metal particles, Rev. Mod. Phys., 58, 533-606 (1986).

[54] Taha, A. and Ahmed, HM., Spectral, Electrochemical and Molecular Orbital Studies on a New Solvatochromic Binuclear Mixed Ligand Copper(II) Complexes, Modern Chem. & Applications,3(3), 1-8 (2015).

[55] Abboud, J.L.M. and Notario, R., Critical compilation of scales of solvent parameters. Part I. pure non-hydrogen bond donor solvents- technical report,Pure Appl. Chem.,71, 645-718 (1999).

[56a] Taha, A., Ramadan, A.A.T., El-Behairy, M.A., Ismail, A.I. and Mahmoud, M.M.,Preferential solvation studies using the solvatochromicdicyanobis(1,10-phenanthroline)iron(II) complex,New J. Chem.,25, 1306-1312 (2001).

[56b] Taha, A. and Kiwan, A.M., Preferential solvation and molecular orbital calculations studies of solvatochromicmesoionic 2,3-diaryl-2H-tetrazolium-5-thiolate,New J. Chem.,25, 502-508 (2001). calculation studies of solvatochromicmesoionic 2,3-diaryl-2H-tetrazolium-5-thiolate calculation studies of solvatochromic mesoionic 2,3-diaryl-2H-tetrazolium-5-thiolate calculation studies of solvatochromicmesoionic 2,3-diaryl-2H-tetrazolium -5-thiolate

[57] Reichardt, C. "Solvents and Solvent Effects in Organic Chemistry"; VCH, Weinheim, 1988.

[58] Habibi-Yangjeh, A., A Model for Correlation of Various Solvatochromic Parameters withComposition in Aqueous and Organic Binary Solvent Systems, Bull. Korean Chem. Soc., 25(8), 1165-1170 (2004).

[58b] Rosés, M.; Buhvestov, U.; Ràfols, C.; Rived, F.; Bosch, E. Solute–solvent and solvent–solvent interactions in binary solvent mixtures. Part 6.A quantitative measurement of the enhancement of the water structure in 2-methylpropan-2-ol–water and propan-2-ol–water mixtures by solvatochromic indicators. J. Chem. Soc. Perkin Trans. 2 1997, 1341–1348

[58c] Rosés, M.; Buhvestov, U.; Ràfols, C.; Rived, F.; Bosch, E. Solute–solvent and solvent–solvent interactions in binary solvent mixtures. Part 6.A quantitative measurement of the enhancement of the water structure in 2-methylpropan-2-ol–water and propan-2-ol–water mixtures by solvatochromic indicators. J. Chem. Soc. Perkin Trans. 2 1997, 1341–1348

[58d] Rosés, M.; Buhvestov, U.; Ràfols, C.; Rived, F.; Bosch, E. Solute–solvent and solvent–solvent interactions in binary solvent mixtures. Part 6.A quantitative measurement of the enhancement of the water structure in 2-methylpropan-2-ol–water and propan-2-ol–water mixtures by solvatochromic indicators. J. Chem. Soc. Perkin Trans. 2 1997, 1341–1348

[58e] Rosés, M.; Buhvestov, U.; Ràfols, C.; Rived, F.; Bosch, E. Solute–solvent and solvent–solvent interactions in binary solvent mixtures. Part 6.A quantitative measurement of the enhancement of the water structure in 2-methylpropan-2-ol–water and propan-2-ol–water mixtures by solvatochromic indicators. J. Chem. Soc. Perkin Trans. 2 1997, 1341–1348

[59] Taha, A., Farag, A.A.M., Adly, O.M.I., Roushdy, N., Shebl, M. and Ahmed, H.M., Photoresponse and DFT studies of new synthesized 2-benzylidene-3-hydroxy -1-(5,6-diphenyl-1,2,4-triazine-3-yl) hydrazine and optical sensor application, *J. Mol. Struct.*, 1142, 66-72 (2017).